

Ultraviolet emission efficiency enhancement of a-plane AlGaN/GaN multiple-quantum-wells with increasing quantum well thickness

Huei-Min Huang, Chiao-Yun Chang, Yu-Pin Lan, Tien-Chang Lu, Hao-Chung Kuo, and Shing-Chung Wang

Citation: *Applied Physics Letters* **100**, 261901 (2012); doi: 10.1063/1.4730438

View online: <http://dx.doi.org/10.1063/1.4730438>

View Table of Contents: <http://scitation.aip.org/content/aip/journal/apl/100/26?ver=pdfcov>

Published by the *AIP Publishing*

Articles you may be interested in

[Exciton recombination dynamics in a -plane \(Al,Ga\)N/GaN quantum wells probed by picosecond photo and cathodoluminescence](#)

J. Appl. Phys. **107**, 043524 (2010); 10.1063/1.3305336

[Optical polarization anisotropy of a -plane GaN/AlGaN multiple quantum well structures grown on r -plane sapphire substrates](#)

J. Appl. Phys. **105**, 123112 (2009); 10.1063/1.3156688

[Well-width dependence of photoluminescence emission from a-plane GaN/AlGaN multiple quantum wells](#)

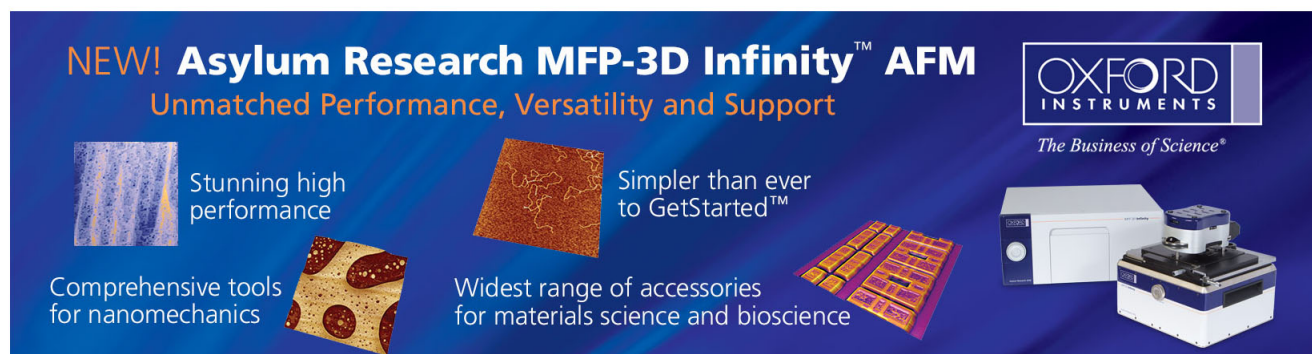
Appl. Phys. Lett. **84**, 496 (2004); 10.1063/1.1638884

[Room-temperature ultraviolet emission from GaN/AlN multiple-quantum-well heterostructures](#)

Appl. Phys. Lett. **83**, 3486 (2003); 10.1063/1.1623335

[GaN/AlGaN multiple quantum wells on a-plane GaN pillars for stripe-geometry nonpolar ultraviolet light-emitting devices](#)

Appl. Phys. Lett. **83**, 2599 (2003); 10.1063/1.1614835

The advertisement features a dark blue background with white and orange text. At the top left, it reads 'NEW! Asylum Research MFP-3D Infinity™ AFM' in large white letters, followed by 'Unmatched Performance, Versatility and Support' in orange. On the right, the Oxford Instruments logo is shown with the tagline 'The Business of Science®'. Below the text are four images: a blue textured surface, a brown textured surface, a grid of colorful squares, and the MFP-3D Infinity AFM instrument itself. Text descriptions are placed around these images: 'Stunning high performance' next to the blue surface, 'Simpler than ever to GetStarted™' next to the brown surface, 'Comprehensive tools for nanomechanics' next to the colorful grid, and 'Widest range of accessories for materials science and bioscience' next to the AFM instrument.

Ultraviolet emission efficiency enhancement of *a*-plane AlGaN/GaN multiple-quantum-wells with increasing quantum well thickness

Huei-Min Huang, Chiao-Yun Chang, Yu-Pin Lan, Tien-Chang Lu,^{a)} Hao-Chung Kuo, and Shing-Chung Wang

Department of Photonics and Institute of Electro-Optical Engineering, National Chiao Tung University, Hsinchu 300, Taiwan

(Received 1 May 2012; accepted 7 June 2012; published online 25 June 2012)

The defect-induced carrier localization in nonpolar *a*-plane (Al,Ga)N/GaN multiple quantum wells (MQWs) structures with different well thickness have been investigated. A strong variation of temperature-dependent photoluminescence peak energy was observed and attributed to the existence of the localized states. The degree of carrier localization in these defect-induced states was more prominent in the case of MQWs with the wider well width. In addition, the ultraviolet light emission efficiency revealed a 3-fold enhancement with increasing the well width from 1.6 nm to 7.3 nm, due to the strong carrier localization generated from the quantum-wire-like features formed by the intersection between basal stacking faults and quantum wells. © 2012 American Institute of Physics. [<http://dx.doi.org/10.1063/1.4730438>]

Wurtzite GaN grown along the nonpolar [11-20] *a*-axis is believed as an effective way to realize the elimination of the internal electric fields, which is induced in GaN-based quantum well structures grown along the [0001] *c*-axis.¹⁻³ In *a*-plane GaN-based materials, the large densities of extended defects such as the intrinsic I_1 -type basal stacking faults (BSFs) are usually observed,^{4,5} due to the lower formation energy in the direction perpendicular to the *c*-axis [0001]. Based on the previous studies,⁶⁻¹⁰ these BSFs were commonly considered to exist in an ultrathin layer (8 Å of 3–4 monolayers) and were made of smooth insertion of the zincblende (ZB) *ABCABC* sequence embedded in the wurtzite (WZ) *ABAB* sequence matrix. Such a structure forms a type-II heterojunction so that the stacking faults are able to behave like a quantum-well-like region of ZB materials surrounded by the WZ host, giving rise to a luminescence line below the WZ bandgap. Recently, the electrical and optical characteristics of BSFs in nonpolar GaN-based materials were attracted more attention. Interestingly, Corfdir *et al.* suggested that localized electrons along BSFs plane were the origin of BSF-bound excitons,¹¹ and the further quantum-wire-like structures could be formed where BSFs intersected with the QWs.¹² Jönen *et al.* then indicated that the quantum-wire-like region formed by stacking faults intersecting with quantum wells could facilitate highly efficient light emission in the nonpolar InGaN/GaN multiple quantum wells (MQWs) structures, due to the efficient carrier confinement.¹³ Baik *et al.* also suggested that the output powers of nonpolar *a*-plane (In,Ga)N light emitting diodes (LEDs) were significantly influenced by the presence of BSFs.¹⁴ Therefore, the effects of BSFs in nonpolar GaN-based materials were regarded as an indispensable factor in light emission.

In this work, the BSFs-induced effects in nonpolar *a*-plane AlGaN/GaN MQWs structure with different well thickness have been studied. With increasing the well width,

the stacking faults intersecting with the QWs dominated the optical properties of these structures and the stacking faults-induced carrier localization became stronger, demonstrated by temperature-dependent photoluminescence measurements. Additionally, the ultraviolet (UV) light emission efficiencies were enhanced in the wider well width, due to the increased degree of carrier localization. And the relationships between the carrier localization and nanostructure in the (Al,Ga)N MQWs were discussed in detail.

The five samples in this study were grown on *r*-plane sapphire substrates by a low-pressure metal organic chemical vapor deposition (EMCORE-D75) system. The ten period *a*-plane Al_{0.17}GaN_{0.83}/GaN MQWs were grown in atmosphere of N₂ at 1100 °C on a 1.5 μm thick GaN template. All samples were grown under identical growth conditions except for the quantum well thickness. In all samples, the barrier thickness was 10 nm, and the well thicknesses were 1.6, 2.4, 3.4, 5.2, and 7.3 nm, respectively. Taking a sample as a representative case, the related defect distribution and real well thickness were estimated by using the transmission electron microscopy (TEM), as shown in Fig. 1. The defect distribution of AlGaN/GaN MQWs was observed by the cross section TEM images along the [1100]_{GaN} zone axis orientation. The BSFs are clearly observed as thin lines aligning in parallel with [0001]_{GaN} *c*-axis direction and propagate from below the GaN epilayer grown on a foreign substrate towards AlGaN barriers and GaN quantum wells. The high-resolution x-ray diffraction (HRXRD) was utilized to quantify the Al composition of AlGaN barrier and the structural strain distribution.¹⁵ For optical measurements, all samples were pumped by a 266 nm pulse laser with an excitation power of 5 mW, generated by a frequency tripled mode-locked Ti: sapphire laser (Mira 900). The luminescence was dispersed by a 0.55 m monochromator with the 2400 grooves/mm grating and detected by a high sensitivity photomultiplier tube for UV-visible wavelengths.

Figure 2(a) shows the low-temperature PL spectra of AlGaN/GaN MQWs with different well thicknesses, and the

^{a)} Author to whom correspondence should be addressed. E-mail: timtclu@mail.nctu.edu.tw. Tel.: +886-3-571-2121 ext. 31234.

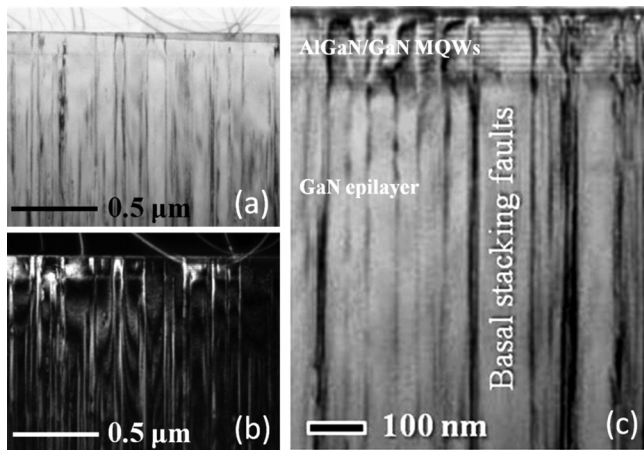


FIG. 1. (a) Bright- and (b) dark-field TEM images of an a -plane AlGaIn/GaN MQWs sample with 3.4 nm well thickness taken along the $[1100]_{\text{GaN}}$ zone axis in the same region. The intersection of BSFs and MQWs is observed in (c).

intensity of main emission peaks increases with the well thickness. In addition, a weak emission peak (around 3.4 eV) located at the low energy side of the main peak could be assigned to the excitons bound to BSFs in the underlying GaN template. Due to the absence of polarization field in nonpolar MQWs, the emission linewidth became much narrower in the wider well samples.¹⁶ According to the previous investigation results,^{12,17} the origins of the main emission peaks in our samples could base on two transition processes, including the recombination of excitons in GaN QWs and in the region where the BSFs intersected with QWs. Therefore, the PL spectra of MQWs samples were fitted with two Gaussian-type distribution peaks to illustrate the influence of QWs emission and BSFs-related emission, respectively. Figure 2(b) shows the peak energy variation of these two emission processes as a function of well thickness and exhibits the red shift with increasing the well thickness. Since the BSFs-related emission process occurred in a quantum wire-like structure, which the dimension of quantum confinement for carriers was higher than that in the QW, the quantized energy states for the BSFs-related emission was more susceptible to the spatial variation of the quantum confined structure. As a consequence, the energy separation between the QWs emission and BSFs-related emission was getting larger in the wider quantum wells as shown in Fig. 2(b). The lower energy states of these quantum wire-like structures

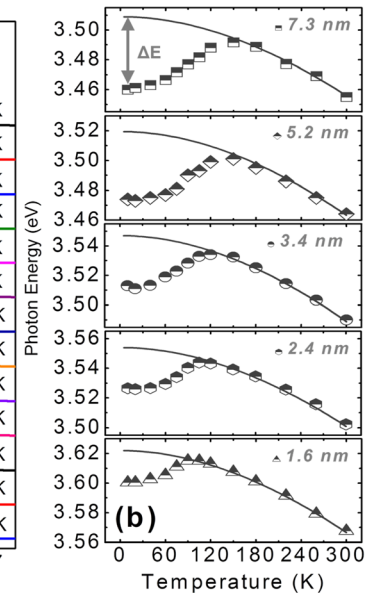
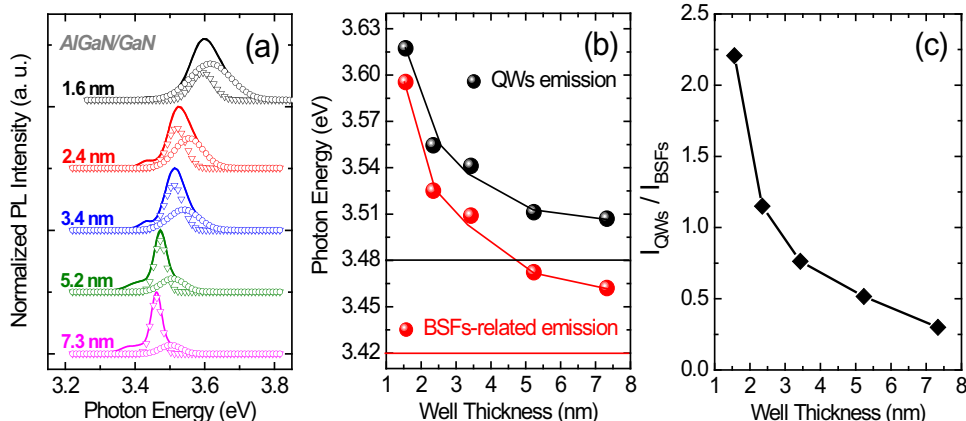


FIG. 3. (a) Temperature-dependent PL spectra of AlGaIn/GaN MQWs with 7.3 nm well thickness. (b) The emission energies at temperature ranging from 10 to 300 K for the different well thicknesses. The solid lines are the fit of the data with the Varshni's formula, and the symbols stand for the measurement data.

could serve as localization centers in the a -plane AlGaIn/GaN QWs. The intensity ratio of QWs emission to BSFs-related emission was denoted as $I_{\text{QWs}}/I_{\text{BSFs}}$, where I_{QWs} and I_{BSFs} were the fitted PL integrated intensity for the QWs and BSFs-related emissions, respectively. The estimated ratio was from 2.2 to 0.3 with increasing the well thickness, shown in Fig. 2(c). The intensity of GaN QWs emission was gradually reduced with increasing the well thickness, and the BSFs-related emission became dominant in the PL spectra.

Temperature-dependent PL spectra ranging from 10 to 300 K of a -plane AlGaIn/GaN MQWs with a 7.3 nm well thickness are shown in Fig. 3(a). A strong variation of the emission peak was observed obviously with increasing the temperature. PL emission peaks showed a blue shift in the temperature range from 10 to 150 K, and a red shift for 150–300 K. An S-shaped emission peak variation as a function of the temperature was a typical indication of the carrier localization behavior. It was implied that the BSFs-related states, originated from the quantum-wire-like region where the BSFs intersected with the QWs, could account for the localization behaviors of carriers in a -plane AlGaIn/GaN

FIG. 2. (a) Low-temperature PL spectra of AlGaIn/GaN MQWs with different well thicknesses, fitted based on two Gaussian-type distribution functions (open symbol), illustrating the influence of BSFs-related emission (low energy) and QWs emission (high energy), respectively. (b) BSFs-related emission and QWs emission lines as a function of the well thickness, and (c) the integrated intensity ratio of these two emission lines, summarizing as a function of the well thickness.

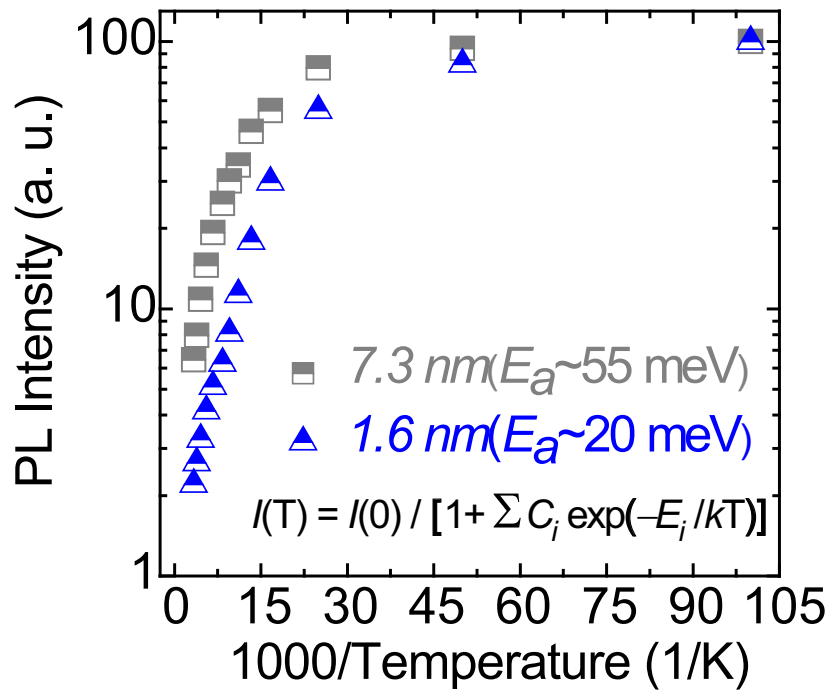


FIG. 4. The normalized PL intensities for AlGaIn/GaN MQWs with 1.6 and 7.3 nm well thicknesses plot as a function of $1/T$. The symbols stand for the measurement data, fitting by Arrhenius equation to investigate the carrier localization behavior during the thermal processes.

MQWs. Figure 3(a) shows that the BSFs-related emission dominates in the temperature range of 10–90 K. The temperature dependence of the MQWs emission peaks with different well thickness can be well fitted by the Varshni's empirical formula as shown in Fig. 3(b). The energy deviations between the fitting curves and experimental data at the lowest measurement temperatures could be regarded as the localized energies of carriers in the BSFs-related states. The localized energy, ΔE , increased with the well thickness from 20 to 51 meV, which could be attributed to the increased energy separation between BSFs and the QWs states when the well thickness increased.

Arrhenius plots of the integrated PL intensities as a function of inverse temperature for a -plane AlGaIn/GaN MQWs samples are shown in Fig. 4. The thermal activation energies can be determined by the equation $I(T) = I(0) / [1 + \sum C_i \exp(-E_i/kT)]$. Values of activation energies were summarized in Table I, and they were increased from 20 to 55 meV with increasing the well thickness. The wider well thickness exhibited the slower thermal quenching and the large activation energy. It is believed that the MQWs with better carrier confinement capability should exhibit greater resistance to thermal quenching of luminescence and have larger activation energy. And the thermal activation energy

TABLE I. Summary of the optical properties at 10 K for $\text{Al}_{0.17}\text{Ga}_{0.83}\text{N}/\text{GaIn}$ MQWs with different well thickness.

Sample	Optical properties at 10 K			
Thickness (nm)	Ratio of I_{MQWs}/I_{BSFs}	Activation energy (E_a , meV)	Localized energy (ΔE , meV)	Light efficiency (η)
1.6	2.20	20	20	2.2%
2.4	1.15	26	27	3.3%
3.4	0.76	35	35	3.6%
5.2	0.51	44	46	4.6%
7.3	0.30	55	51	6.5%

plays an important role as the degree of confined potential preventing carriers to escape or delocalize. The experimental results showed that the a -plane AlGaIn/GaN MQWs with wider well thickness would have better carrier confinement capability, which was in accordance with the above measurement results. In addition, the light emission efficiency, based on the definition of temperature-dependent PL, also increased with the well thickness. The related optical properties at 10 K for a -plane AlGaIn/GaN MQWs with different well thickness are summarized in Table I. The UV light emission efficiency revealed a 3-fold enhancement with increasing the well width from 1.6 nm to 7.3 nm. The enhancement of the light emission efficiency may be due to the BSFs-induced strong carrier localization behavior and then result in strong radiative recombination processes. Moreover, the thermal activation energy was almost identical with the carrier localized energy for all samples, and thus, the thermal quenching process could reasonably be attributed to the carriers delocalization from the BSFs-induced localized states in the QWs. The origin of light emission efficiency enhancement due to the BSFs-induced effect in the (Al,Ga)N/GaN MQWs seemed to be very similar to the influence of In-rich nanoscale clusters for (In,Ga)N/GaN MQWs.¹⁸ According to the results, the BSFs-induced strong carrier localization indeed enhanced the light emission efficiency in a -plane AlGaIn/GaN MQWs structures and affected the optical properties with increasing the well thickness.

In conclusion, the relationships between the BSFs-induced effects and well thickness in a -plane (Al,Ga)N/GaN MQWs structures have been studied. The BSFs-related emission dominated the low temperature PL spectra in the wider well thickness. The MQWs with wider well thickness showed a better carrier confinement and strong carrier localization, due to the formation of BSFs-induced localized states. In addition, the 3-fold enhancement of the UV light emission efficiency with increasing the well width from

1.6 nm to 7.3 nm was observed due to the consequence of the strong carrier localization behavior.

This work was supported by the MOE ATU program and in part by the National Science Council of Republic of China (ROC) in Taiwan under contract NSC-99-2120-M-009-007 and NSC 99-2221-E-009-035-MY3.

- ¹M. D. Craven, S. H. Lim, F. Wu, J. S. Speck, and S. P. DenBaars, *Appl. Phys. Lett.* **81**, 1201 (2002).
- ²T. S. Ko, T. C. Wang, R. C. Gao, H. G. Chen, G. S. Huang, T. C. Lu, H. C. Kuo, and S. C. Wang, *J. Cryst. Growth* **300**, 308 (2007).
- ³S. C. Ling, C. L. Chao, J. R. Chen, P. C. Liu, T. S. Ko, T. C. Lu, H. C. Kuo, S. C. Wang, S. J. Cheng, and J. D. Tsay, *J. Cryst. Growth* **312**, 1316 (2010).
- ⁴B. A. Haskell, F. Wu, M. D. Craven, s. Matsuda, P. T. Fini, T. Fujii, K. Fujito, S. P. DenBaars, J. S. Speck, and S. Nakamura, *Appl. Phys. Lett.* **83**, 644 (2003).
- ⁵D. N. Zakharov, Z. Liliental-Weber, B. Wagner, Z. J. Reitmeier, E. A. Preble, and R. F. Davis, *Phys. Rev. B* **71**, 235334 (2005).
- ⁶C. Stampfl and C. G. Van de Walle, *Phys. Rev. B* **57**, R15052 (1998).
- ⁷G. Salviati, M. Albrecht, C. Zanotti-Fregonara, N. Armani, M. Mayer, Y. Shreter, M. Guzzi, Y. V. Melnik, K. Vassilevski, V. A. Dmitiev, and H. P. Strunk, *Phys. Status Solidi A* **171**, 325 (1999).
- ⁸R. Liu, A. Bell, F. A. Ponce, C. Q. Chen, J. W. Yang, and M. A. Khan, *Appl. Phys. Lett.* **86**, 021908 (2005).
- ⁹X. Ni, U. Özgür, Y. Fu, N. Biyikli, J. Xie, A. A. Baski, H. Morkoç, and Z. Liliental-Weber, *Appl. Phys. Lett.* **89**, 262105 (2006).
- ¹⁰P. Corfdir, P. Lefebvre, J. Levrat, A. Dussaigne, J. D. Ganière, D. Martin, J. Ristić, T. Zhu, N. Grandjean, and B. Deveaud-Plédran, *J. Appl. Phys.* **105**, 043102 (2009).
- ¹¹P. Corfdir, P. Lefebvre, J. Ristić, J. D. Ganière, and B. Deveaud-Plédran, *Phys. Rev. B* **80**, 153309 (2009).
- ¹²P. Corfdir, P. Lefebvre, L. Balet, S. Sonderegger, A. Dussaigne, T. Zhu, D. Martin, J. D. Ganière, N. Grandjean, and B. Deveaud-Plédran, *J. Appl. Phys.* **107**, 043524 (2010).
- ¹³H. Jönen, U. Rossow, H. Bremers, L. Hoffmann, M. Brendel, A. D. Dräger, S. Schwaiger, F. Scholz, J. Thalmair, J. Zweck, and A. Hangleiter, *Appl. Phys. Lett.* **99**, 011901 (2011).
- ¹⁴K. H. Baik, Y. G. Seo, S. K. Hong, S. Lee, J. Kim, J. S. Son, and S. M. Hwang, *IEEE Photon. Technol. Lett.* **22**(5), 595 (2010).
- ¹⁵H. M. Huang, C. Y. Chang, T. C. Lu, and C. C. Yang, *J. Electrochem. Soc.* **158**, H915 (2011).
- ¹⁶D. Bimberg, J. Christen, T. Fukunaga, H. Nakashima, D. E. Mars, and J. N. Miller, *J. Vac. Sci. Technol. B* **5**, 1191 (1987).
- ¹⁷T. J. Badcock, P. Dawson, M. J. Kappers, C. McAleese, J. L. Hollander, C. F. Johnston, D. V. Sridhara Rao, A. M. Sanchez, and C. J. Humphreys, *Appl. Phys. Lett.* **93**, 101901 (2008).
- ¹⁸J. H. Na, R. A. Taylor, K. H. Lee, T. Wang, A. Tahraoui, P. Parbrook, A. M. Fox, S. N. Yi, Y. S. Park, J. W. Choi, and J. S. Lee, *Appl. Phys. Lett.* **89**, 253120 (2006).